The Long Non-coding RNA LINC01133 Promotes Hepatocellular Carcinoma Progression by Sponging miR-199a-5p and Activating Annexin A2

Dan Yin
Fudan University IBS: Fudan University Institutes of Biomedical Sciences
Zhi-Qiang Hu
Zhongshan Hospital Fudan University Department of Liver Surgery
Chu-Bin Luo
Zhongshan Hospital Fudan University Department of Liver Surgery
Xiao-Yi Wang
Liver Cancer Institute, Zhongshan Hospital, Fudan University
Hao-Yang Xin
Zhongshan Hospital Fudan University Department of Liver Surgery
Rong-Qi Sun
Zhongshan Hospital Fudan University Department of Liver Surgery
Peng-Cheng Wang
Zhongshan Hospital Fudan University Department of Liver Surgery
Jia Fan
Zhongshan Hospital Fudan University Department of Liver Surgery
Jian Zhou
Zhongshan Hospital Fudan University Department of Liver Surgery
Zheng-Jun Zhou
Zhongshan Hospital Fudan University Department of Liver Surgery
Shaolai Zhou (zhoushaolai99@sina.com)
Zhongshan Hospital Fudan University Department of Liver Surgery https://orcid.org/0000-0002-8526-5221

Research

Keywords: LINC01133, hepatocellular carcinoma, miR-199a-5p, Annexin A2, EMT

Posted Date: December 22nd, 2020

DOI: https://doi.org/10.21203/rs.3.rs-130867/v1

Abstract

Background: Long non-coding RNAs (lncRNAs) have been found to be functionally associated with cancer development and progression. Although copy number variations (CNVs) are common in hepatocellular carcinoma (HCC), little is known about how CNVs in lncRNAs affect HCC progression and recurrence.

Methods: We analyzed the whole genome sequencing (WGS) data of matched cancerous and non-cancerous liver samples from 49 patients with HCC to identify lncRNAs with CNVs. The results were validated in another cohort of 238 paired HCC and non-tumor samples by TaqMan copy number assay. Kaplan-Meier analysis and the log-rank test were performed to determine the prognostic value of CNVs in lincRNAs. Loss- and gain-of-function studies were conducted to determine the biological functions of LINC01133 in vitro and in vivo. The competing endogenous RNAs (ceRNAs) mechanism was clarified by microRNA sequencing (miR-seq), quantitative real-time PCR (qRT-PCR), western blot, and dual-luciferase reporter analyses. The protein binding mechanism was confirmed by RNA pull-down, RNA immunoprecipitation (RIP), qRT-PCR, and western blot analyses.

Results: Genomic copy number of LINC01133 was increased in HCC, which is positively related with the elevated expression of LINC01133. Increased copy number of LINC01133 predicted the poor prognosis in HCC patients. LINC01133 overexpression promoted proliferation, colony formation, migration, and invasion in vitro, and facilitated tumor growth and lung metastasis in vivo, whereas LINC01133 knockdown had the opposite effects. Mechanistically, LINC01133 acted as a sponge of miR-199a-5p, resulting in enhanced expression of SNAI1, which induced epithelial-mesenchymal transition (EMT) in HCC cells. In addition, LINC01133 interacted with Annexin A2 (ANXA2) to activate ANXA2/STAT3 signaling pathway.

Conclusions: LINC01133 promotes HCC progression by sponging miR-199a-5p and interacting with ANXA2. LINC01133 CNV gain is predictive of poor prognosis in HCC patients undergoing curative resection.

Background

Hepatocellular carcinoma (HCC) is a common cancer that is usually not diagnosed until it reaches late stages of development, leading to poor prognosis and a 5-year survival rate below 50% [1, 2]. Distant metastasis and tumor recurrence are common in patients with HCC [3, 4]. HCC development and progression involve complex genetic and epigenetic changes [5–7]. Thus, it is critical to understand those changes to identify reliable prognostic predictors and therapeutic targets.

Copy number variation (CNV) is a type of structural variants involving the genomic nucleotide sequences alterations (deletion or amplification) in the specific regions of DNA [8]. CNV plays critical roles in cancer development and progression by activating oncogenes and inactivating tumor suppressors. Protein-coding genes only account for 2% of the human genome, and numerous CNVs appear at a high

frequency in populations are located in the non-coding gene regions [9]. Long non-coding RNAs (lncRNAs) are at least 200 nucleotides in length and do not encode any protein [10]. Mounting studies have demonstrated that lncRNAs function in many biological processes, including epigenetic, transcriptional, and post-transcriptional regulation [11–13]. LncRNAs exert regulatory functions in human disease development by binding to microRNAs (miRNAs) and suppressing miRNA-mediated gene silencing [14]. There is accumulating evidence that dysregulation of lncRNAs is involved in human cancers, including HCC [15]. CNV affects lncRNA expression and can predict tumor prognosis [16]. Long intergenic non-coding RNAs (lincRNAs) have no overlap with any other genes and are the most common type of lncRNA [17]. Therefore, it is of vital importance to explore the role of transcriptional dysregulation caused by CNVs in lincRNAs during HCC progression and recurrence.

We analyzed whole genome sequencing (WGS) data from our previous study to screen for lincRNAs with CNVs involved in HCC recurrence after curative resection [18]. We examined CNVs and expression levels of candidate lincRNAs in HCC tissue samples. We then investigated the relationship between CNVs in lincRNAs and HCC outcomes. Finally, we explored the biological roles of LINC01133 and the mechanisms by which it promotes HCC progression.

Methods

Patients and follow up

This study included two independent cohorts comprising a total of 287 patients with HCC (cohort1, n = 49; cohort 2, n = 238). The patient characteristics are summarized in **Supplementary Table 1**. Details regarding the patients and follow up are given in the Supplementary Information.

Statistical analysis

Statistical analysis was conducted using SPSS 20.0 (Chicago, IL, USA) for Windows or GraphPad Prism V7 (GraphPad, La Jolla, CA, USA). Measured values were expressed as the mean ± standard deviation (SD). Normally distributed data were analyzed using two-tailed Student's-t test or analysis of variance. Categorical variables were compared using Chi-square test or Pearson’s test. Correlation between two variables was analyzed using Pearson’s coefficient. Relationships with clinicopathological characteristics were analyzed by Chi-square test or Fisher’s exact test. The Kaplan-Meier method followed by log-rank test was used for survival analysis. We considered P values < 0.05 statistically significant.

Other Materials And Methods

Please refer to the Supplementary Information for more details regarding the materials and methods used.

Results

Identification of LINC01133 with CNVs involved in HCC recurrence and prognosis

We revealed a genome-wide heatmap of CNVs in lncRNAs determined by WGS data of 49 Chinese patients with HCC who underwent curative resection and subsequently experienced HCC recurrence (cohort 1; Fig. 1A; **Supplementary Fig. 1A**) [18]. LncRNAs that were frequently amplified were mainly located on chromosomes 1q, 8q, 17q, 20q, whereas those that were frequently deleted were mainly located on chromosomes 4q, 9q, 13q, and 16q (Fig. 1A). We selected seven lincRNAs (LINC00051, LINC00303, LINC00482, LINC00862, LINC01133, LINC01136, and LINC01300) that had average copy number > 3.0 and CNV gain in > 50% of the HCC samples for further investigation (Fig. 1B, **Supplementary Table 2**). To verify the CNVs of these lincRNAs, we analyzed an additional 238 pairs of human HCC tumors and adjacent non-tumor tissue samples (cohort 2) by TaqMan copy number assay. The results confirmed that the copy numbers of all seven candidate lincRNAs were higher in the tumors than in the matched non-tumor tissues (Fig. 1C and 1D). We also measured the expression levels of the seven lincRNAs in 70 pairs of tumor and non-tumor samples randomly selected from cohort 2 and found that the expression levels of LINC00482 ($P < 0.001$), LINC00862 ($P = 0.0014$) and LINC01133 ($P = 0.0086$) were significantly higher in the tumor samples than in the matched non-tumor samples (Fig. 1E; **Supplementary Fig. 1B**). We did not detect significant differences in the expression levels of the other four candidate lincRNAs between the tumor and non-tumor samples (**Supplementary Fig. 1B**).

We analyzed the association between CNVs in these seven lincRNAs and clinical outcomes in cohort 2. The 238 patients were categorized into two groups: CNV^{high} and CNV^{low} according to each lincRNA CNVs (**Supplementary Fig. 1C**). Kaplan-Meyer analysis showed that CNVs gain in LINC01133 and LINC01300 were associated with reduced overall survival (OS; Fig. 1F, **left panel; Supplementary Fig. 1D**). Because both the genomic copy numbers and the RNA expression levels of LINC01133 were elevated in HCC tissues compared with those in matched non-tumor tissues, we selected LINC01133 for further investigation. Patients with high LINC01133 copy numbers in their tumors exhibited shorter tumor-free survival than those with low LINC01133 copy numbers in their tumors (Fig. 1F, **right panel**). Univariate and multivariate analyses suggested that LINC01133 CNV was an independent prognostic factor for patient survival (Tables 1 and 2). In addition, the LINC01133 CNV was positively correlated with the LINC01133 relative expression level in the tumors compared with non-tumor tissues (Fig. 1G). RNAscope assay confirmed that LINC01133 was overexpressed in HCC tumors compared with the adjacent non-tumor tissues and mainly existed in cytoplasm of the tumor cells **(**Fig. 1H). Collectively, our results demonstrated that LINC01133 was frequently amplified at the genomic-sequence and overexpressed at transcript levels in the tumors of patients that experienced HCC, implying that LINC01133 plays a role in HCC recurrence and prognosis.

Table 1
Correlation between the factors and clinicopathologic characteristics in HCC (Cohort 2, n = 238)

Clinicopathological Indexes		CNV in LINC01133		*P* value*
		Lower(n = 138)	High(n = 100)	
Age(year)	≤ 50	59	50	0.268
	> 50	79	50	
Sex	Female	22	10	0.185
	Male	116	90	
HBsAg	Negative	20	13	0.742
	Positive	118	87	
AFP (ng/ml)	≤ 20	48	36	0.846
	> 20	90	64	
GGT(U/L)	≤ 54	62	35	0.124
	> 54	76	65	
Liver cirrhosis	No	35	19	0.247
	yes	103	81	
Tumor size(cm)	≤ 5	70	44	0.305
	> 5	68	56	
Tumor number	Single	117	83	0.711
	Multiple	21	17	
Microvascular invasion	Absence	126	88	0.403
	Present	12	12	
Tumor encapsulation	None	55	40	0.982
	Complete	83	60	
Tumor differentiation**	I + II	95	59	0.117
	III + IV	43	41	

* Chi-square tests for all analyses. ** Edmondson grade. Abbreviations: CNV, copy number variation; HBsAg, hepatitis B surface antigen; AFP, alpha-fetoprotein; GGT, gamma-glutamyl transpeptidase.

Table 2
Univariate and multivariate analyses of prognostic factors in HCC (Cohort 2, n = 238)

Variable	OS		TTR	
	HR (95% CI)	*P*	HR (95% CI)	*P*
Univariate analysis*				
Age, year (≤ 50 vs.>50)	0.942(0.661–1.341)	0.739	1.053(0.770–1.439)	0.746
Sex (female vs. male)	1.375(0.788–2.399)	0.262	1.040(0.663–1.631)	0.866
HBsAg (negative vs. positive)	0.820(0.485–1.387)	0.460	0.551(0.333–0.912)	**0.020**
AFP, ng/ml (≤ 20 vs.>20)	1.284(0.880–1.875)	0.195	1.145(0.826–1.589)	0.416
GGT, U/L (≤ 54 vs.>54)	1.710(1.172–2.494)	**0.005**	1.187(0.863–1.631)	0.292
Liver cirrhosis (no vs. yes)	1.405(0.893–2.210)	0.142	1.349(0.907–2.007)	0.139
Tumor size, cm (≤ 5 vs.>5)	2.927(2.003–4.279)	**0.000**	2.090(1.518–2.879)	**0.000**
Tumor number (single vs. multiple)	1.178(0.742–1.868)	0.487	1.206(0.801–1.814)	0.369
Microvascular invasion (no vs. yes)	2.713(1.639–4.490)	**0.000**	2.000(1.235–2.241)	**0.005**
Tumor encapsulation (complete vs. none)	0.839(0.587–1.199)	0.336	0.752(0.550–1.029)	0.075
Tumor differentiation** (I + II vs. III + IV)	1.620(1.130–2.322)	**0.009**	1.201(0.868–1.661)	0.269
CNV in LINC01133 (low vs. high)	1.616(1.136–2.299)	**0.008**	1.399(1.024–1.910)	**0.035**
Multivariate analysis*				
HBsAg (negative vs. positive)	NA	NA	0.533(0.321–0.886)	**0.015**

*Analyses were conducted using univariate analysis or multivariate Cox proportional hazards regression; **Edmondson grade. *P* values less than 0.05 were considered statistically significant. Boldface type indicates significant values. Abbreviations: OS, overall survival; TTR, time to recurrence; AFP, alpha-fetoprotein; HBsAg, hepatitis B surface antigen; GGT, gamma-glutamyl transpeptidase; HR, hazard ratio; CI, confidential interval; CNV: copy number variation.

Variable	OS		TTR	
	HR (95% CI)	*P*	HR (95% CI)	*P*
GGT, U/L (≤ 54 vs.>54)	1.314(0.891–1.937)	0.168	NA	NA
Tumor size, cm (≤ 5 vs.>5)	3.097(2.081–4.609)	**0.000**	2.138(1.549–2.949)	**0.000**
Microvascular invasion (no vs. yes)	2.581(1.530–4.355)	**0.000**	2.182(1.337–3.563)	**0.002**
Tumor differentiation** (I + II vs. III + IV)	1.634(1.130–2.363)	**0.009**	NA	NA
CNV in LINC01133 (low vs. high)	1.522(1.065–2.176)	**0.021**	1.337(0.978–1.828)	0.068

*Analyses were conducted using univariate analysis or multivariate Cox proportional hazards regression; **Edmondson grade. *P* values less than 0.05 were considered statistically significant. Boldface type indicates significant values. Abbreviations: OS, overall survival; TTR, time to recurrence; AFP, alpha-fetoprotein; HBsAg, hepatitis B surface antigen; GGT, gamma-glutamyl transpeptidase; HR, hazard ratio; CI, confidential interval; CNV: copy number variation.

Characteristics And Distribution Of Linc01133 In Hcc Cell Lines

LINC01133 is located in chromosome 1q23.2 (**Supplementary Fig. 2A**) without protein-encoding ability (https://lncipedia.org/; **Supplementary Table 3**). We detected copy numbers and expression level of LINC01133 in HCC cell lines with different metastatic potentials. We found that the LINC01133 copy numbers and expression levels were both greater in HCC cell lines with high metastatic potential (MHCC97H, MHCC97L, and HCCLM3) than in HCC cells lines with low metastatic potential (Hep3B, PLC/PRF/5, Huh7, and HepG2; Fig. 2A and 2B). RNAscope assays showed that LINC01133 was more highly expressed in MHCC97H cells than in HepG2 cells and mainly existed in the cytoplasm in both cell lines (Fig. 2C). Likewise, quantitative real-time PCR (qRT-PCR) revealed that LINC01133 was localized to the cytoplasm and the nucleus of MHCC97H and HCCLM3 cells, both of which had high overall expression of LINC01133, but was relatively enriched in the cytoplasm in both cell lines (Fig. 2D).

LINC01133 promotes HCC cell proliferation, migration, and invasion in vitro and in vivo

We utilized short hairpin RNA (shRNA) to knock down LINC01133 expression in HCCLM3 and MHCC97H cells. In addition, we used lentivirus-based expression vectors to overexpress LINC01133 in HepG2 and PLC/PRF/5 cells. We confirmed the knockdown and overexpression of LINC01133 in the respective cell lines by qRT-PCR and agarose gel electrophoresis (Fig. 3A). Compared with corresponding control cells, cells overexpressing LINC01133 had increased rates of proliferation and colony formation, whereas cells

with LINC01133 knockdown had reduced rates of proliferation and colony formation (Fig. 3B and 3C). Similarly, cell migration and invasion assays showed that cells overexpressing LINC01133 had increased cell numbers of migration and invasion compared with control cells, whereas those with LINC01133 knockdown had reduced cell numbers of migration and invasion compared with control cells (Figs. 3D and 3E).

The mouse xenograft model showed that PLC/PRF/5 cells overexpressing LINC01133 produced larger tumors and more metastatic lung nodules than PLC/PRF/5 cells expressing the empty vector. Conversely, MHCC97H cells with LINC01133 knockdown produced smaller tumors and fewer metastatic lung nodules than MHCC97H cells expressing a control shRNA (Fig. 3F). These data suggested that LINC01133 promotes HCC cells growth and metastasis in vitro and in vivo.

LINC01133 acts as a sponge of miR-199a-5p in HCC cells

LincRNAs in the cytoplasm can potentially act as sponges to inactivate miRNAs and thus regulate the post-transcriptional translation of target genes [14]. To determine if LINC01133 can sponge miRNAs to affect HCC development and progression, we performed miRNA sequencing (miR-seq) in HCC cells with LINC01133 overexpression and LINC01133 silencing. Among 1620 known miRNAs appearing in one or more of the HCC cell lines, we identified 94 miRNAs that were down-regulated (fold-change > 2) in PLC/PRF/5 cells overexpressing LINC01133 in comparison with control cells, 149 miRNAs that were up-regulated (fold-change > 2) in MHCC97H cells with LINC01133 silencing in comparison with control cells, and 422 miRNAs that were predicted by the miRanda miRNA Target Prediction Tool to bind to LINC01133 (Fig. 4A and 4B). Two miRNAs, miR-199a-5p and miR-501-5p, were included in all three groups (Fig. 4B). qRT-PCR showed that LINC01133 overexpression reduced miR-199a-5p levels, but not miR-501-5p levels, in PLC/PRF/5 cells (Fig. 4C). Conversely, LINC01133 knockdown enhanced miR-199a-5p expression, but not miR-501-5p expression, in MHCC97H cells compared to control cells (Fig. 4C). Analysis using the miRanda software revealed sequence complementary to miR-199-5p at nucleotide (nt) positions 961–983 of LINC01133 (Fig. 4D). In dual-luciferase reporter gene assays, miR-199a-5p inhibited the luciferase reporter activity of wild-type LINC01133 but not that of mutant LINC01133 (Fig. 4D). These data indicated that LINC01133 sponges miR-199a-5p in HCC cells.

LINC01133 triggers epithelial-mesenchymal transition (EMT) in HCC cells through miR-199a-5p/snail signaling

It has been reported that miR-199a-5p binds to the 3'-UTR (untranslated region) of SNAI1 to inhibit its expression [19, 20]. In agreement with previous study, the complementary sequence of miR-199a-5p was identified in the 3’-UTR of SNAI1 mRNA by TargetScan 7.0 (http://targetscan.org; **Supplementary Fig. 2B**). Luciferase reporter assays showed that miR-199a-5p overexpression suppressed the luciferase-reported activity of the wild-type SNAI1 3'-UTR, but not that of a mutant SNAI1 3'-UTR (**Supplementary Fig. 2B**). It was well known that snail is a key transcription factor linked to EMT. Therefore, we examined the expression of snail and markers related to EMT in HCC cells with LINC01133 overexpression or knockdown by qRT-PCR and western blot. We found that LINC01133 overexpression in PLC/PRF/5 cells

up-regulated the mRNA and protein levels of snail, vimentin, and N-cadherin, whereas LINC01133 knockdown in MHCC97H cells attenuated the mRNA and proteins levels of those EMT markers (Figs. 4E and 4F). We observed the inverse results for E-cadherin expression (Figs. 4E and 4F).

For further investigation, we performed rescue experiments to investigate whether LINC01133 regulates EMT in an miR-199a-5p-dependent manner. We transfected LINC01133-overexpressing PLC/PRF/5 cells with a miR-199a-5p lentiviral vector. We then transfected LINC01133-silenced MHCC97H cells with an anti-miR-199a-5p lentiviral vector and measured the expression of miR-199a-5p in the cells by qRT-PCR (Fig. 4G). We found that overexpression of miR-199a-5p up-regulated E-cadherin expression and down-regulated snail, vimentin, and N-cadherin expression in the LINC01133-overexpressing PLC/PRF/5 cells (Fig. 4H and 4I). Conversely, in the LINC01133-silenced MHCC97H cells, anti-miR-199a-5p down-regulated E-cadherin expression and up-regulated snail, vimentin, and N-cadherin expression (Fig. 4H and 4I). Together, those results suggested that LINC01133 regulates EMT in HCC cells in a miR-199a-5p/snail dependent manner.

Linc01133 Activates Anxa2/stat3/cyclin D1 Signaling In Hcc Cells

In addition to interacting with other RNAs, lincRNAs also exert functions by interacting directly with proteins. We performed RNA pull-down assays to identify LINC01133-associated proteins. Mass spectrometry analysis of a ~ 35 KD protein band pulled down by LINC01133 (Fig. 5A) revealed nine potential LINC01133 binding proteins, excluding keratin, with peptide number > 5 and unique peptide number > 5 (Fig. 5B). Of the nine potential LINC01133 binding proteins, ANXA2 had the highest total score in protein identification analysis (Fig. 5B and 5C). We verified the presence of ANXA2 among the proteins isolated in the RNA pull-down assay by western blot (Fig. 5D). The RNAfold database (http://rna.tbi.univie.ac.at/cgi-bin/RNAWebSuite/RNAfold.cgi) and Cat-Rapid database (http://service.tartaglialab.com/page/catrapid_omics_group) consistently predicted that ANXA2 possibly binds to 126–177nt or 651-792nt of LINC01133 (**Supplementary Fig. 2C and 2D**). Moreover, RNA immunoprecipitation (RIP) assays showed that LINC01133 was enriched in lysates of MHCC97H cells treated with anti-ANXA2 antibody in comparison with lysates of MHCC97H cells treated with IgG protein (Fig. 5E), further confirming the interaction between LINC01133 and ANXA2 in HCC cells.

To further investigate the possible role of the LINC01133/ANXA2 signaling axis in HCC, we measured the expression of ANXA2 by qRT-PCR and western blot. The results showed that the mRNA level of ANXA2 was not affected by LINC01133 overexpression in PLC/PRF/5 cells or by LINC01133 silencing in MHCC97H cells (Fig. 5F). By contrast, the protein level of ANXA2 was increased by LINC01133 overexpression in PLC/PRF/5 cells and reduced by LINC01133 silencing in MHCC97H cells (Fig. 5G). Furthermore, LINC01133 overexpression increased the phosphorylation levels of ANXA2 and STAT3 and the expression level of cyclinD1 in PLC/PRF/5 cells, whereas LINC01133 silencing reduced the phosphorylation levels of ANXA2 and STAT3 and the expression level of cyclinD1 in MHCC97H cells

(Fig. 5G). Taken together, our results confirmed that LINC01133 interacts with ANXA2 to activate STAT3/cyclin D1 signaling, which may be involved in the proliferation of HCC induced by this lincRNA.

Discussion

Genomic and molecular phenotype heterogeneity due to CNV is thought to influence HCC development and progression [21]. Many CNVs have been identified in intergenic regions of DNA in human HCC cells [22]. In this study, based on WGS and bioinformatics analyses of 49 matched HCC samples and para-cancer tissues, the genomic CNVs of lncRNAs in Chinese patients with HCC who had early tumor recurrence after curative resection were revealed for the first time. In a previous study, Yang et al. identified frequent deletions in 147 lncRNAs, such as FENDRR, that are recurrently deregulated in HCC [23]. Li et al. identified frequent amplifications in the oncogenic lncRNA LINC01138 in HCC and showed that the amplifications were associated with poor disease outcomes [24]. Zhou et al. reported that CNV in the lncRNA-PRAL was a crucial stimulus for HCC growth and might provide an effective target for antitumor therapy [25]. We found that LINC01133 copy numbers and expression were elevated in HCC samples compared with those in matched non-tumor tissues. In addition, we found that LINC01133 CNVs and RNA expression levels were positively correlated with each other in HCC samples, suggesting that LINC01133 increased copy number is at least partially responsible for LINC01133 up-regulation in HCC. Furthermore, LINC01133 CNV gain was predictive of early HCC recurrence and poor prognosis after curative surgery. Those findings suggest that CNV in LINC01133 plays a role in HCC recurrence and prognosis.

There is accumulating evidence that the downstream targets and signaling pathways regulated by LINC01133 are involved in the malignant behavior of multiple types of cancer cells [26-29]. In non-small cell lung carcinoma, LINC01133 suppresses the transcription of KLF2, P21 and E-cadherin by binding to EZH2 and LSD1, resulting in increased cell growth and invasion [30]. In colon cancer, LINC01133 inhibits EMT and metastasis via interaction with SRSF6 [31]. In osteosarcoma, LINC01133 promotes tumor growth as an miR-422a sponge [28]. In this study, we revealed that LINC01133 promotes proliferation, colony formation, migration, and invasion in HCC cells and facilitates HCC growth and metastasis in mouse xenograft models. Further, we explored the underlying mechanism of LINC01133 on HCC progression.

LincRNAs interact with proteins, miRNAs, and other molecules to exert their functions [32]. Previous studies suggested that LINC01133 sponges miR-4784 and miR-205 to counter microRNA-mediated gene silencing in cervical cancer and gastric cancer, respectively [33, 34]. We revealed that LINC01133 is a sponge of miR-199a-5p in HCC through miR-seq and bioinformatics analyses. Additionally, we found that SNAI1 is a target of miR-199a-5p, which is consistent with the results of a previous study [19]. Rescue assays confirmed that LINC01133 up-regulated snail expression by interacting directly with miR-199a-5p. EMT is well known to play a key role in tumor invasion and metastasis [35]. Features of EMT are gain of mesenchymal markers, such as vimentin and N-cadherin, and loss of epithelial cell-junction proteins, such as E-cadherin, in subsets of cancer cells [36]. We reported that high LINC01133 expression in HCC

cells was correlated with high vimentin and N-cadherin expression and low E-cadherin expression, furthermore, that LINC01133 induced EMT in HCC cells by sponging miR-199a-5p.

in non-small-cell lung cancer [26,27], colorectal cancer [28] and osteosarcoma [29]. It could promote NSCLS cells' proliferation, migration and invasion through binding to EZH2 and LSD1 to repress KLF2, P21 and E-cadherin transcription [27]. As in colorectal cancer, LINC01133 inhibits epithelial-mesenchymal transition and metastasis by directly binding to SRSF6 [28]. LINC01133 could also sponge miR-422a to aggravate the tumorigenesis of human osteosar-coma [29].

LINC01133 has been reported in non-small-cell lung cancer [26,27], colorectal cancer [28] and osteosarcoma [29]. It could promote NSCLS cells' proliferation, migration and invasion through binding to EZH2 and LSD1 to repress KLF2, P21 and E-cadherin transcription [27]. As in colorectal cancer, LINC01133 inhibits epithelial-mesenchymal transition and metastasis by directly binding to SRSF6 [28]. LINC01133 could also sponge miR-422a to aggravate the tumorigenesis of human osteosar-coma [29].

LincRNAs can interact with proteins to regulate gene expression at post-translational level. LINC01133 exerts oncogenic functions in nasopharyngeal carcinoma and lung cancer by binding to YBX1 and EZH2, respectively [30, 37]. We revealed that LINC01133 hound to ANXA2 to promote its expression. Several studies demonstrated that Tyr23 phosphorylation of ANXA2 involves enhancing cancer proliferation and metastasis [38, 39]. ANXA2 also regulates glioma cell proliferation via the STAT3-cyclinD1 pathway [40]. We found that LINC01133 increased the phosphorylation levels of ANXA2 and STAT3 and up-regulated the downstream target gene cyclinD1 in HCC, which might account for its effects on HCC cell proliferation.

Conclusion

LINC01133 CNV gain is predictive of poor prognosis in patients with HCC. LINC01133 promotes HCC progression by sponging miR-199a-5p to enhance snail expression, resulting in enhanced EMT. LINC01133 can also interact with ANXA2 to activate STAT3/cyclinD1 signaling. Therefore, LINC01133 might be a new indicator for progression and prognosis, and a potential therapeutic target in HCC.

Abbreviations

HCC: hepatocelluar carcinoma; CNV: copy number variation; lncRNA: long non-coding RNA; lincRNA: long intergenic non-coding RNA; WGS: whole genome sequencing; OS: overall survival; EMT: epithelial-mesenchymal transition; ANXA2: Annexin A2; qRT-PCR: quantitative real-time polymerase chain reaction; RIP: RNA immunoprecipitation; ceRNA: competing endogenous RNA; ISH: in situ hybridization; miRNA: microRNA; TTR: Time to recurrence; CCK-8: cell-counting-8 kit

Declarations

Acknowledgements

Not applicable.

Authors' contributions

DY, ZQH, CBL, XYW contributed equally to the study. DY, ZQH, CBL and XYW performed the experiments; DY and SLZ analyzed and interpreted the data; HYX, RQS and PCW provided the tissue samples and the clinical data; DY, SLZ and ZJZ drafted the manuscript. JF and JZ commented on the study and revised the paper; ZJZ and SLZ obtained funding and designed the research. All authors read and approved the final manuscript.

Funding

This study was jointly supported by the National Natural Science Foundation of China (No. 82072681, No. 82003082, No. 81773069, No. 81972708), the Shanghai Rising-Star Program (18QA1401200), and the Municipal Human Resources Development Program for Outstanding Young Talents in Medical and Health Sciences in Shanghai (2018YQ14).

Availability of data and materials

All data in our study are available upon request.

Ethics approval and consent to participate

The Research Ethics Committee of Zhongshan Hospital granted ethical approval for the use of human subjects. All participants gave informed consent to be included in the study.

Consent for publication

Not applicable.

Competing interests

The authors declare that they have no competing interests.

References

1. Farazi PA, DePinho RA. Hepatocellular carcinoma pathogenesis: from genes to environment. Nature reviews Cancer. 2006;6(9):674–87. http://doi.org/10.1038/nrc1934.
2. Takayama T. Surgical Treatment for Hepatocellular Carcinoma. Japanese Journal Of Clinical Oncology. 2011;41(4):447–54. http://doi.org/10.1093/jjco/hyr016.
3. Tang ZY, Ye SL, Liu YK, Qin LX, Sun HC, Ye QH, et al. A decade's studies on metastasis of hepatocellular carcinoma. J Cancer Res Clin Oncol. 2004;130(4):187–96. http://doi.org/10.1007/s00432-003-0511-1.

4. Zhou SL, Zhou ZJ, Hu ZQ, Huang XW, Wang Z, Chen EB, et al. Tumor-Associated Neutrophils Recruit Macrophages and T-Regulatory Cells to Promote Progression of Hepatocellular Carcinoma and Resistance to Sorafenib. Gastroenterology. 2016;150(7):1646-58 e17. http://doi.org/10.1053/j.gastro.2016.02.040.
5. Aravalli RN, Steer CJ, Cressman EN. Molecular mechanisms of hepatocellular carcinoma. Hepatology. 2008;48(6):2047–63. http://doi.org/10.1002/hep.22580.
6. Zhou SL, Hu ZQ, Zhou ZJ, Dai Z, Wang Z, Cao Y, et al. miR-28-5p-IL-34-macrophage feedback loop modulates hepatocellular carcinoma metastasis. Hepatology. 2016;63(5):1560–75. http://doi.org/10.1002/hep.28445.
7. Zhou SL, Yin D, Hu ZQ, Luo CB, Zhou ZJ, Xin HY, et al. A Positive Feedback Loop Between Cancer Stem-Like Cells and Tumor-Associated Neutrophils Controls Hepatocellular Carcinoma Progression. Hepatology. 2019;70(4):1214–30. http://doi.org/10.1002/hep.30630.
8. Thapar A, Cooper M. Copy number variation: what is it and what has it told us about child psychiatric disorders? J Am Acad Child Adolesc Psychiatry. 2013;52(8):772–4. http://doi.org/10.1016/j.jaac.2013.05.013.
9. Kung JT, Colognori D, Lee JT. Long noncoding RNAs: past, present, and future. Genetics. 2013;193(3):651–69. http://doi.org/10.1534/genetics.112.146704.
10. Rinn JL, Chang HY. Genome regulation by long noncoding RNAs. Annual review of biochemistry. 2012;81:145–66. http://doi.org/10.1146/annurev-biochem-051410-092902.
11. Monnier P, Martinet C, Pontis J, Stancheva I, Ait-Si-Ali S, Dandolo L. H19 lncRNA controls gene expression of the Imprinted Gene Network by recruiting MBD1. Proc Natl Acad Sci USA. 2013;110(51):20693–8. http://doi.org/10.1073/pnas.1310201110.
12. Chen LL, Carmichael GG. Decoding the function of nuclear long non-coding RNAs. Curr Opin Cell Biol. 2010;22(3):357–64. http://doi.org/10.1016/j.ceb.2010.03.003.
13. Chen ZZ, Huang L, Wu YH, Zhai WJ, Zhu PP, Gao YF. LncSox4 promotes the self-renewal of liver tumour-initiating cells through Stat3-mediated Sox4 expression. Nature communications. 2016;7:12598. http://doi.org/10.1038/ncomms12598.
14. Thomson DW, Dinger ME. Endogenous microRNA sponges: evidence and controversy. Nature reviews Genetics. 2016;17(5):272–83. http://doi.org/10.1038/nrg.2016.20.
15. Spizzo R, Almeida MI, Colombatti A, Calin GA. Long non-coding RNAs and cancer: a new frontier of translational research? Oncogene. 2012;31(43):4577–87. http://doi.org/10.1038/onc.2011.621.
16. Hu X, Feng Y, Zhang D, Zhao SD, Hu Z, Greshock J, et al. A functional genomic approach identifies FAL1 as an oncogenic long noncoding RNA that associates with BMI1 and represses p21 expression in cancer. Cancer cell. 2014;26(3):344–57. http://doi.org/10.1016/j.ccr.2014.07.009.
17. Cabili MN, Trapnell C, Goff L, Koziol M, Tazon-Vega B, Regev A, et al. Integrative annotation of human large intergenic noncoding RNAs reveals global properties and specific subclasses. Genes Dev. 2011;25(18):1915–27. http://doi.org/10.1101/gad.17446611.

18. Zhou S-L, Zhou Z-J, Hu Z-Q, Song C-L, Luo Y-J, Luo C-B, et al. Genomic sequencing identifies WNK2 as a driver in hepatocellular carcinoma and a risk factor for early recurrence. J Hepatol. 2019;71(6):1152–63. http://doi.org/10.1016/j.jhep.2019.07.014.
19. Ma S, Jia W, Ni S. miR-199a-5p inhibits the progression of papillary thyroid carcinoma by targeting SNAI1. Biochemical and biophysical research communications. 2018;497(1):181–6. http://doi.org/10.1016/j.bbrc.2018.02.051.
20. Yi M, Liu B, Tang Y, Li F, Qin W, Yuan X. Irradiated Human Umbilical Vein Endothelial Cells Undergo Endothelial-Mesenchymal Transition via the Snail/miR-199a-5p Axis to Promote the Differentiation of Fibroblasts into Myofibroblasts. BioMed research international. 2018;2018:4135806. http://doi.org/10.1155/2018/4135806.
21. Furuya T, Suehiro Y, Namiki Y, Sasaki K. CNVs Associated with Susceptibility to Cancers: A Mini-Review. Journal of Cancer Therapy. 2015;06(05):413–22. http://doi.org/10.4236/jct.2015.65044.
22. Gu DL, Chen YH, Shih JH, Lin CH, Jou YS, Chen CF. Target genes discovery through copy number alteration analysis in human hepatocellular carcinoma. World journal of gastroenterology. 2013;19(47):8873–9. http://doi.org/10.3748/wjg.v19.i47.8873.
23. Yang Y, Chen L, Gu J, Zhang H, Yuan J, Lian Q, et al. Recurrently deregulated lncRNAs in hepatocellular carcinoma. Nature communications. 2017;8:14421. http://doi.org/10.1038/ncomms14421.
24. Li Z, Zhang J, Liu X, Li S, Wang Q, Di C, et al. The LINC01138 drives malignancies via activating arginine methyltransferase 5 in hepatocellular carcinoma. Nature communications. 2018;9(1). http://doi.org/10.1038/s41467-018-04006-0.
25. Zhou CC, Yang F, Yuan SX, Ma JZ, Liu F, Yuan JH, et al. Systemic genome screening identifies the outcome associated focal loss of long noncoding RNA PRAL in hepatocellular carcinoma. Hepatology. 2016;63(3):850–63. http://doi.org/10.1002/hep.28393.
26. Zheng YF, Zhang XY, Bu YZ. LINC01133 aggravates the progression of hepatocellular carcinoma by activating the PI3K/AKT pathway. Journal of cellular biochemistry. 2019;120(3):4172–9. http://doi.org/10.1002/jcb.27704.
27. Huang CS, Chu J, Zhu XX, Li JH, Huang XT, Cai JP, et al. The C/EBPbeta-LINC01133 axis promotes cell proliferation in pancreatic ductal adenocarcinoma through upregulation of CCNG1. Cancer letters. 2018;421:63–72. http://doi.org/10.1016/j.canlet.2018.02.020.
28. Zeng HF, Qiu HY, Feng FB. Long Noncoding RNA LINC01133 Sponges miR-422a to Aggravate the Tumorigenesis of Human Osteosarcoma. Oncology research. 2017. http://doi.org/10.3727/096504017X14907375885605.
29. Feng Y, Qu L, Wang X, Liu C. LINC01133 promotes the progression of cervical cancer by sponging miR-4784 to up-regulate AHDC1. Cancer Biol Ther. 2019;20(12):1453–61. http://doi.org/10.1080/15384047.2019.1647058.
30. Zang C, Nie FQ, Wang Q, Sun M, Li W, He J, et al. Long non-coding RNA LINC01133 represses KLF2, P21 and E-cadherin transcription through binding with EZH2, LSD1 in non small cell lung cancer.

Oncotarget. 2016;7(10):11696–707. http://doi.org/10.18632/oncotarget.7077.

31. Kong J, Sun W, Li C, Wan L, Wang S, Wu Y, et al. Long non-coding RNA LINC01133 inhibits epithelial-mesenchymal transition and metastasis in colorectal cancer by interacting with SRSF6. Cancer letters. 2016;380(2):476–84. http://doi.org/10.1016/j.canlet.2016.07.015.
32. Ulitsky I, Bartel DP. lincRNAs: genomics, evolution, and mechanisms. Cell. 2013;154(1):26–46. http://doi.org/10.1016/j.cell.2013.06.020.
33. Zeng HF, Qiu HY, Feng FB. Long Noncoding RNA LINC01133 Functions as an miR-422a Sponge to Aggravate the Tumorigenesis of Human Osteosarcoma. Oncology research. 2018;26(3):335–43. http://doi.org/10.3727/096504017X14907375885605.
34. Zhang J, Gao S, Zhang Y, Yi H, Xu M, Xu J, et al. MiR-216a-5p inhibits tumorigenesis in Pancreatic Cancer by targeting TPT1/mTORC1 and is mediated by LINC01133. Int J Biol Sci. 2020;16(14):2612–27. http://doi.org/10.7150/ijbs.46822.
35. Yang J, Weinberg RA. Epithelial-mesenchymal transition: at the crossroads of development and tumor metastasis. Dev Cell. 2008 Jun;14(6):818–29. http://doi.org/10.1016/j.devcel.2008.05.009.
36. Serrano-Gomez SJ, Maziveyi M, Alahari SK. Regulation of epithelial-mesenchymal transition through epigenetic and post-translational modifications. Mol Cancer. 2016 Feb 24;15:18. http://doi.org/10.1186/s12943-016-0502-x.
37. Zhang W, Du M, Wang T, Chen W, Wu J, Li Q, et al. Long non-coding RNA LINC01133 mediates nasopharyngeal carcinoma tumorigenesis by binding to YBX1. American journal of cancer research. 2019;9(4):779–90. http://www.ncbi.nlm.nih.gov/pubmed/31106003.
38. Zheng L, Foley K, Fau - Huang L, Huang L, Fau - Leubner A, Leubner A, Fau - Mo G, Mo G, Fau - Olino K, Olino K, Fau - Edil BH, et al. Tyrosine 23 phosphorylation-dependent cell-surface localization of annexin A2 is required for invasion and metastases of pancreatic cancer. PLoS One. 2011 Apr 29;6(4):e19390. http://doi.org/10.1371/journal.pone.0019390.
39. Yuan J, Yang Y, Gao Z, Wang Z, Ji W, Song W, et al. Tyr23 phosphorylation of Anxa2 enhances STAT3 activation and promotes proliferation and invasion of breast cancer cells. Breast cancer research treatment. 2017;164(2):327–40. http://doi.org/10.1007/s10549-017-4271-z.
40. Chen L, Lin L, Xian N, Zheng Z. Annexin A2 regulates glioma cell proliferation through the STAT3cyclin D1 pathway. Oncol Rep. 2019;42(1):399–413. http://doi.org/10.3892/or.2019.7155.

Figures

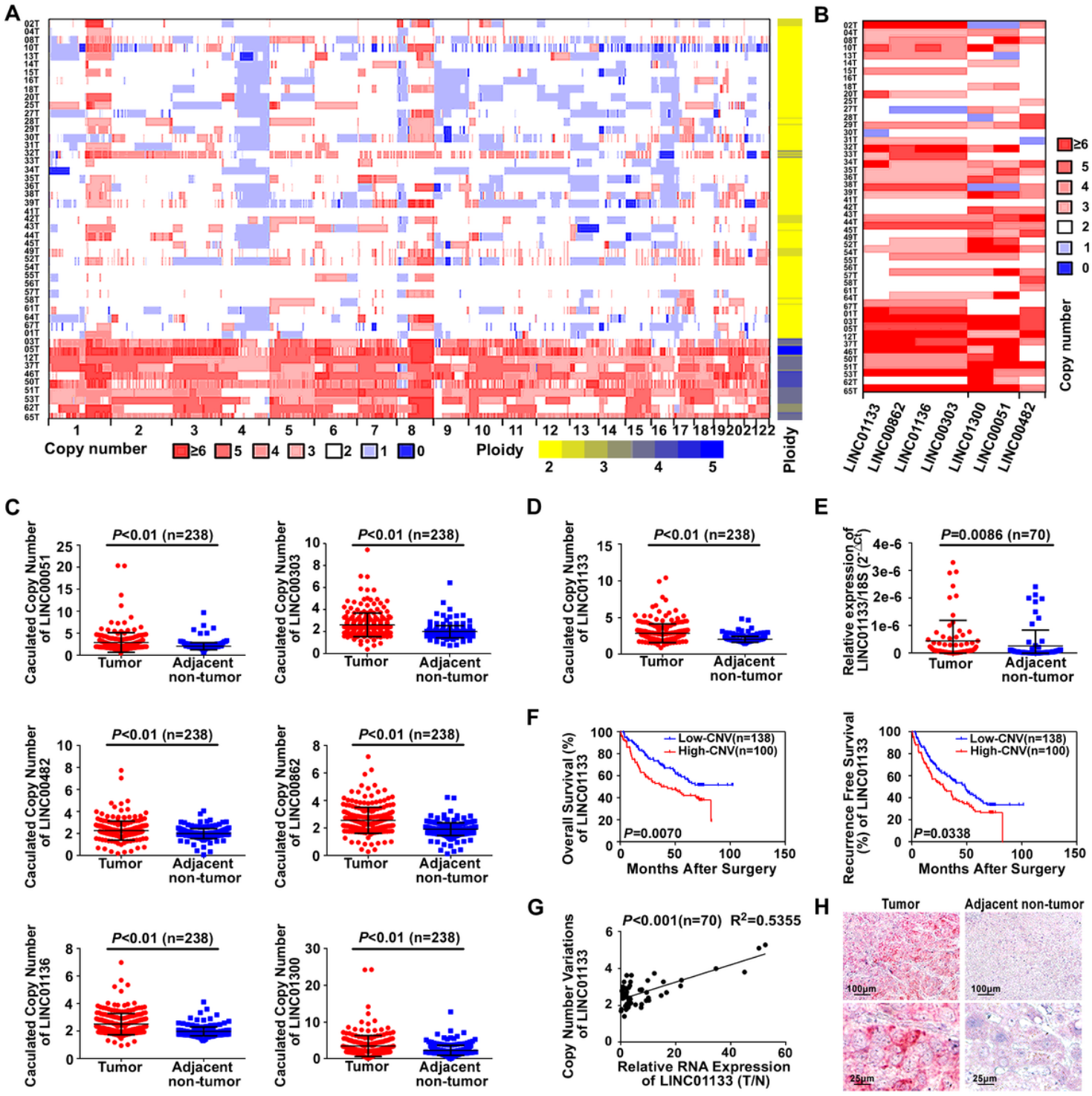

Figure 1

Identification of LINC01133 with CNVs involved in HCC recurrence and prognosis. (A) Heatmaps of genomic CNVs in lncRNAs (cohort 1: n=49). Chromosomal coordinates are on the X-axis. The right band shows the ploidy status. (B) Heatmaps of genomic CNVs in seven selected lincRNAs (LINC00051, LINC00303, LINC00482, LINC00862, LINC01133, LINC01136 and LINC01300). (C) TaqMan copy number assay revealed that copy numbers of six lincRNAs (LINC00051, LINC00303, LINC00482, LINC00862, LINC01136 and LINC01300) were significantly increased in tumor tissues compared with those in

adjacent non-tumor tissues (cohort 2: n=238). RNase P was used as an internal reference. (D) TaqMan copy number assay revealed that copy number of LINC01133 was significantly increased in tumor tissues compared with that in adjacent non-tumor tissues (cohort 2: n=238). RNase P was used as an internal reference. (E) qRT-PCR revealed that LINC01133 expression was increased in tumor tissues compared with that in adjacent non-tumor tissues (n=70). 18S rRNA was used as an internal reference. (F) Kaplan-Meier analysis of OS (left panel) and recurrence-free survival (right panel) of 238 patients based on CNVs in LINC01133 (cohort 2). (G) LINC01133 CNVs and relative expression levels were positively correlated in HCC tissues (n=70), T: tumor tissue. N: adjacent non-tumor tissue. (H) In suit hybridization (ISH) results showed that LINC01133 was high-expressed in tumor tissues and mainly localized in the cytoplasm of HCC cells. Scale bar: 100 μm (upper panel), 25 μm (lower panel).

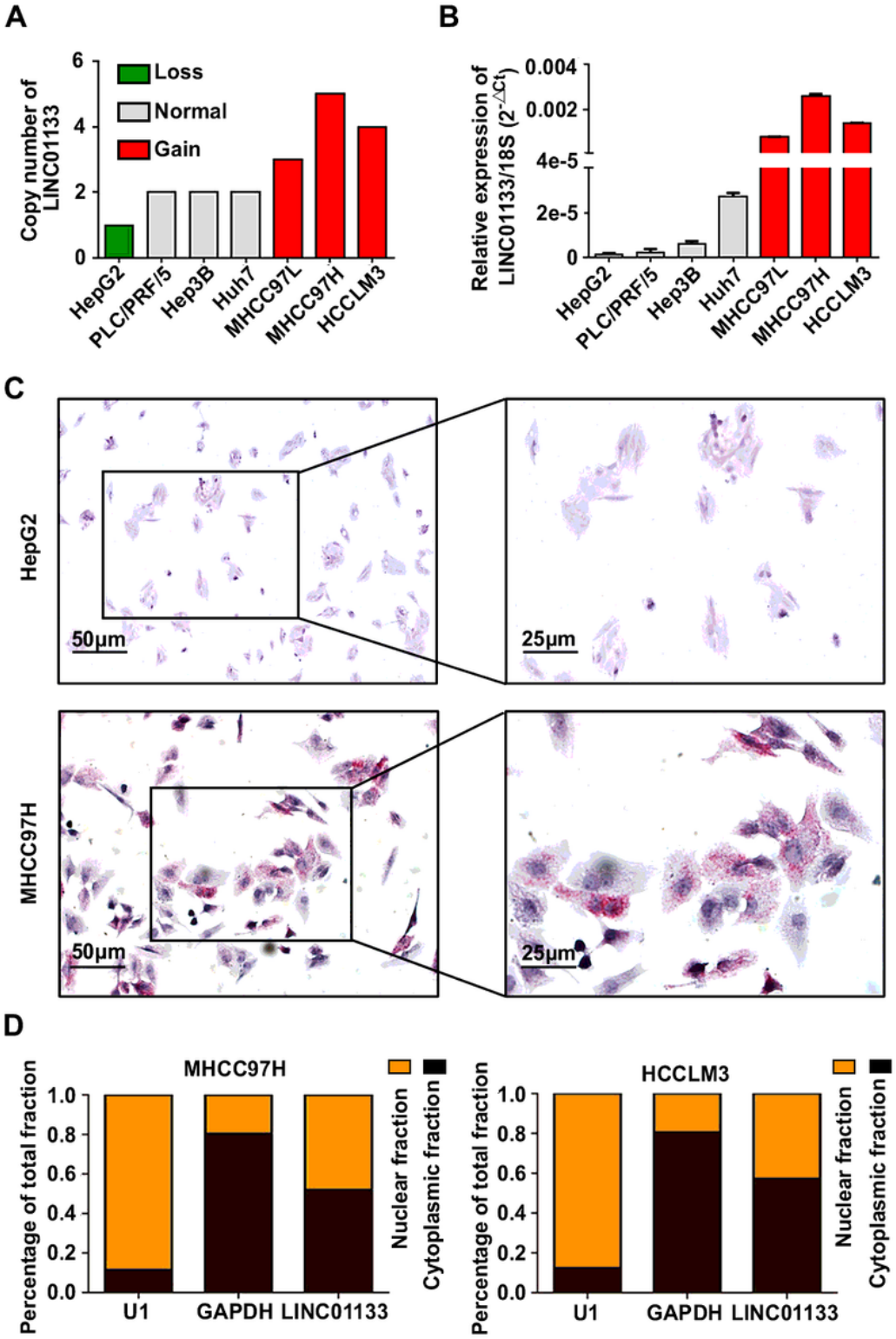

Figure 2

Characteristics and distribution of LINC01133 in HCC cell lines. (A) The copy numbers of LINC01133 in HCC cell lines determined by TaqMan copy number assay. RNase P was used as an internal reference. (B) Relative expression of LINC01133 in HCC cell lines determined by qRT-PCR. 18S rRNA was used as an internal reference. Data are shown as mean ± standard deviation and are representative of three independent experiments. (C) ISH experiments showed the localization and expression of LINC01133 in

HepG2 (upper panel) and MHCC97H cells (lower panel). Scale bar: 50 μm (left panel), 25 μm (right panel). (D) The subcellular localization of LINC01133 was detected by qRT-PCR in MHCC97H and HCCLM3 cells. U1 snRNA was used as a nuclear reference. GAPDH was used as a cytoplasmic reference.

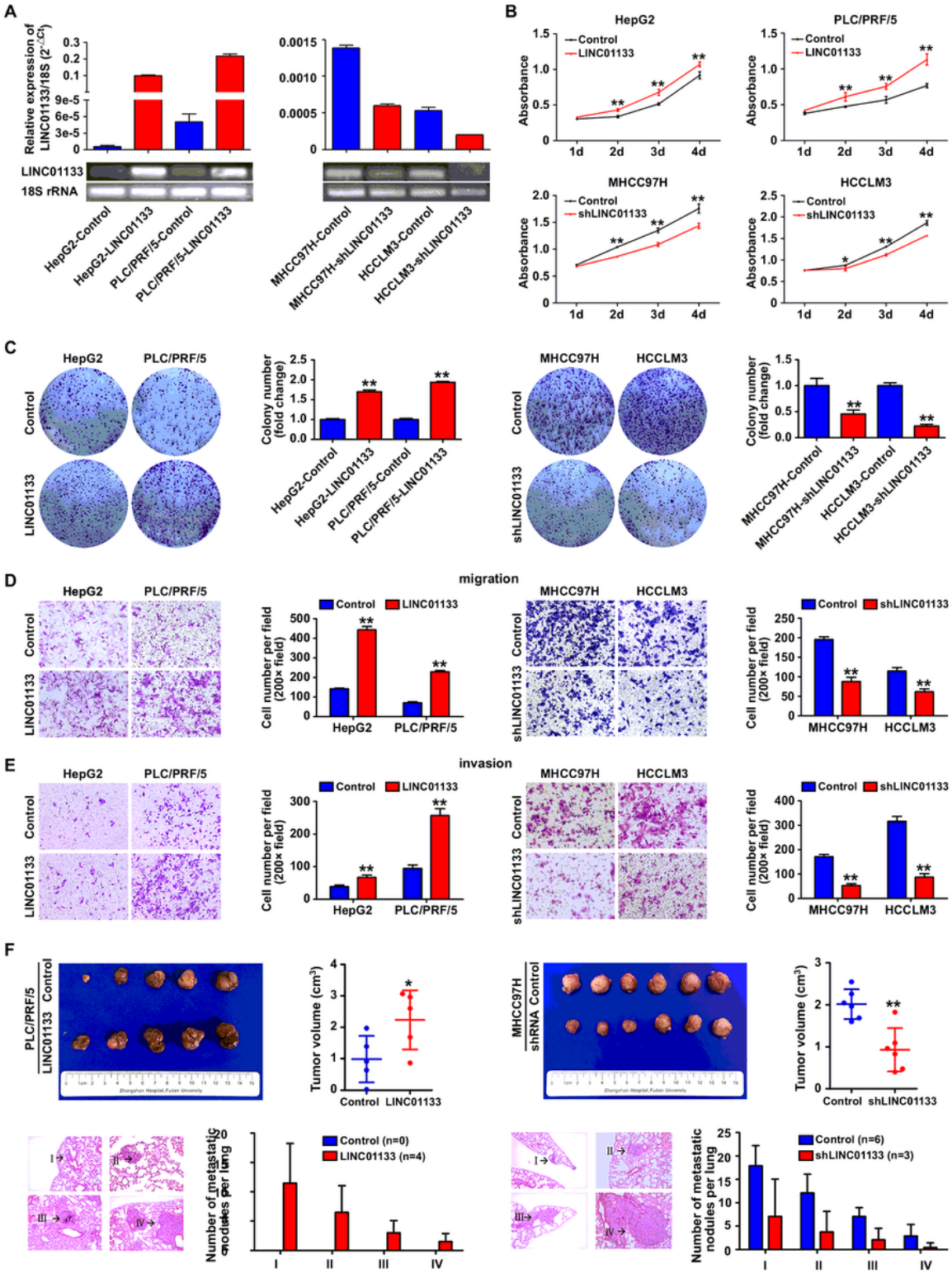

Figure 3

LINC01133 promotes HCC cell proliferation, migration, and invasion in vitro and in vivo. (A) qRT-PCR and agarose gel eletrophoresis assays showed that LINC01133 RNA levels increased in PLC/PRF/5 and

HepG2 cells containing lentivirus-based expression vectors (left panel) and decreased in MHCC97H and HCCLM3 cells transfecting a LINC01133-specific shRNA (right panel). 18S rRNA was used as an internal reference. (B) CCK8 assays showed that LINC01133 overexpression promoted proliferation in HepG2 and PLC/PRF/5 cells (upper panel), whereas LINC01133 silencing inhibited proliferation in MHCC97H and HCCLM3 cells (down panel). *P<0.05, **P<0.01. (C) Colony formation results showed that LINC01133 overexpression promoted colony formation in HepG2 and PLC/PRF/5 cells (left panel), whereas LINC01133 silencing inhibited colony formation in MHCC97H and HCCLM3 (right panel). **P<0.01. (D) Cell migration assays showed that LINC01133 overexpression promoted migration in HepG2 and PLC/PRF/5 cells (left panel), whereas LINC01133 silencing inhibited migration in MHCC97H and HCCLM3 cells (right panel). **P<0.01. (E) Cell invasion assays showed that LINC01133 overexpression promoted invasion in HepG2 and PLC/PRF/5 cells (left panel), whereas LINC01133 silencing inhibited invasion in MHCC97H and HCCLM3 cells (right panel). **P<0.01. (F) Tumor weights of xenografts in the mouse model of HCC (upper panel). Representative images show hematoxylin-eosin staining of metastatic nodules in lungs from different animal groups. The metastases grades in each group are indicated (lower panel). *P<0.05, **P<0.01. Data are shown as the mean ± standard deviation and are representative of three independent experiments.

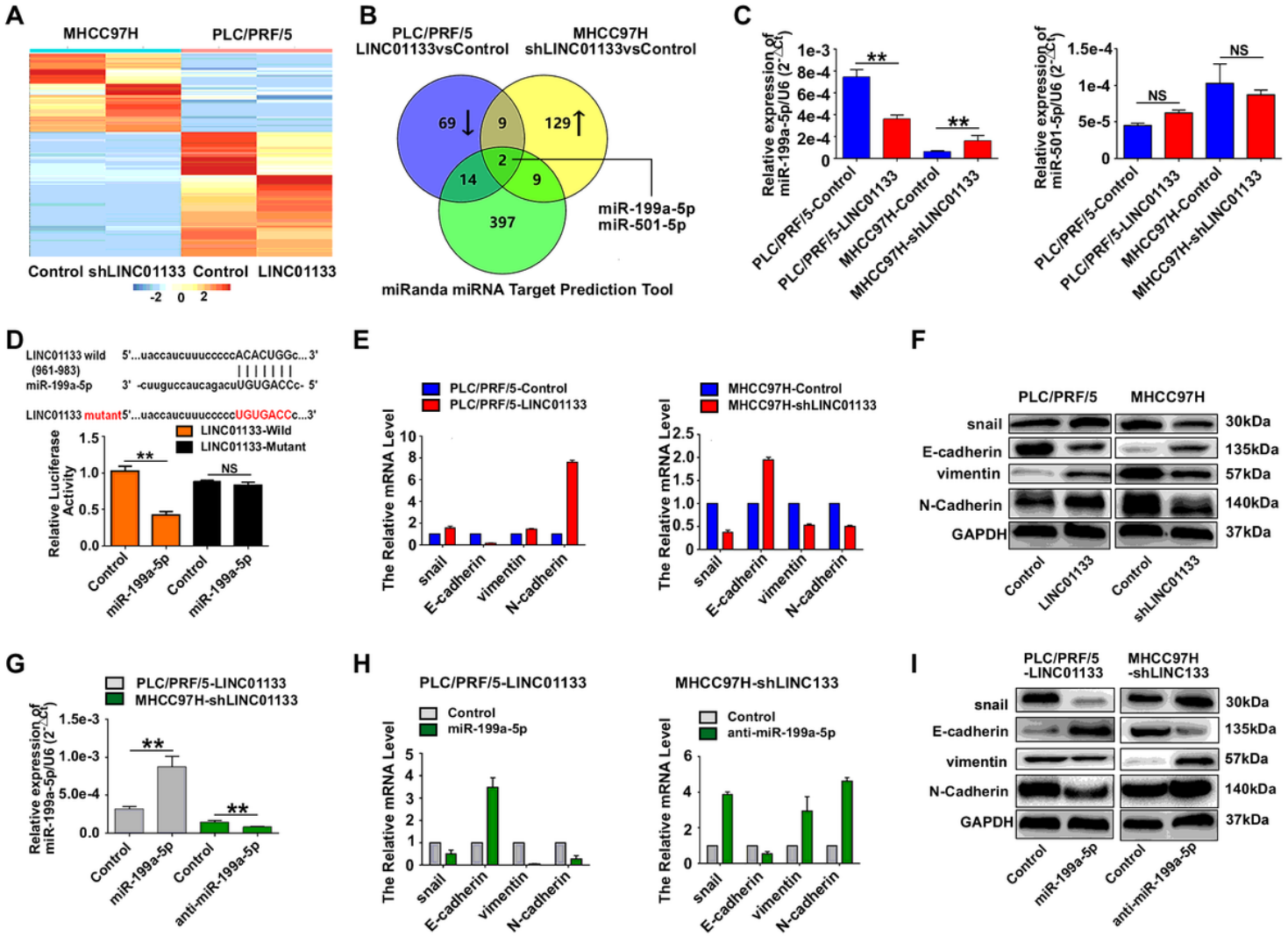

Figure 4

LINC01133 is a sponge of miR-199a-5p and induces EMT in HCC cells. (A) Heatmap of differentially expressed miRNAs in LINC01133-overexpressing PLC/PRF/5 cells vs. control cells and LINC01133-silenced MHCC97H cells vs. control cells, revealed by miR-seq. (B) Venn diagrams show the numbers of miRNAs that potentially binds to LINC01133 according to three groupings: (1) down-regulated miRNAs in PLC/PRF/5 cells after overexpression of LINC01133 (fold change >2); (2) up-regulated miRNAs in MHCC97H cells treated with shLINC01133 vectors (fold change >2); and (3) miRNAs predicted by miRanda miRNA Target Prediction Tool to interact with LINC01133. (C) qRT-PCR was performed to examine the expression of miR-199a-5p (left panel) and miR-501-5p (right panel) in LINC01133-overexpressing PLC/PRF/5 cells and LINC01133-silenced MHCC97H cells. U6 snRNA was used as an internal reference. **P < 0.01. (D) The sequences of miR-199a-5p and its potential binding sites in LINC01133 are shown. The red nucleotides indicate mutant predicted binding sites. Luciferase assays were used to examine the interaction between LINC01133 and miR-199a-5p. **P < 0.01. qRT-PCR (E) and western blot (F) showed changes in snail and EMT-marker expression following stable up-regulation or down-regulation of LINC01133 expression. (G) qRT-PCR was performed to assess the expression of miR-199a-5p in LINC01133-overexpressing PLC/PRF/5 cells and LINC01133-silenced MHCC97H cells following treatment with miR-199a-5p and anti-miR-199a-5p, respectively. U6 snRNA was used as an internal reference. **P < 0.01. qRT-PCR (H) and western blot (I) were conducted to measure mRNA and protein levels of snail, E-cadherin, vimentin and N-cadherin in LINC01133-overexpressing PLC/PRF/5 cells and LINC01133-silenced MHCC97H cells after treatment with miR-199a-5p and anti-miR-199a-5p, respectively. GAPDH was used as an internal reference in qRT-PCR and western blot. Data are shown as the mean ± standard deviation and are representative of three independent experiments.

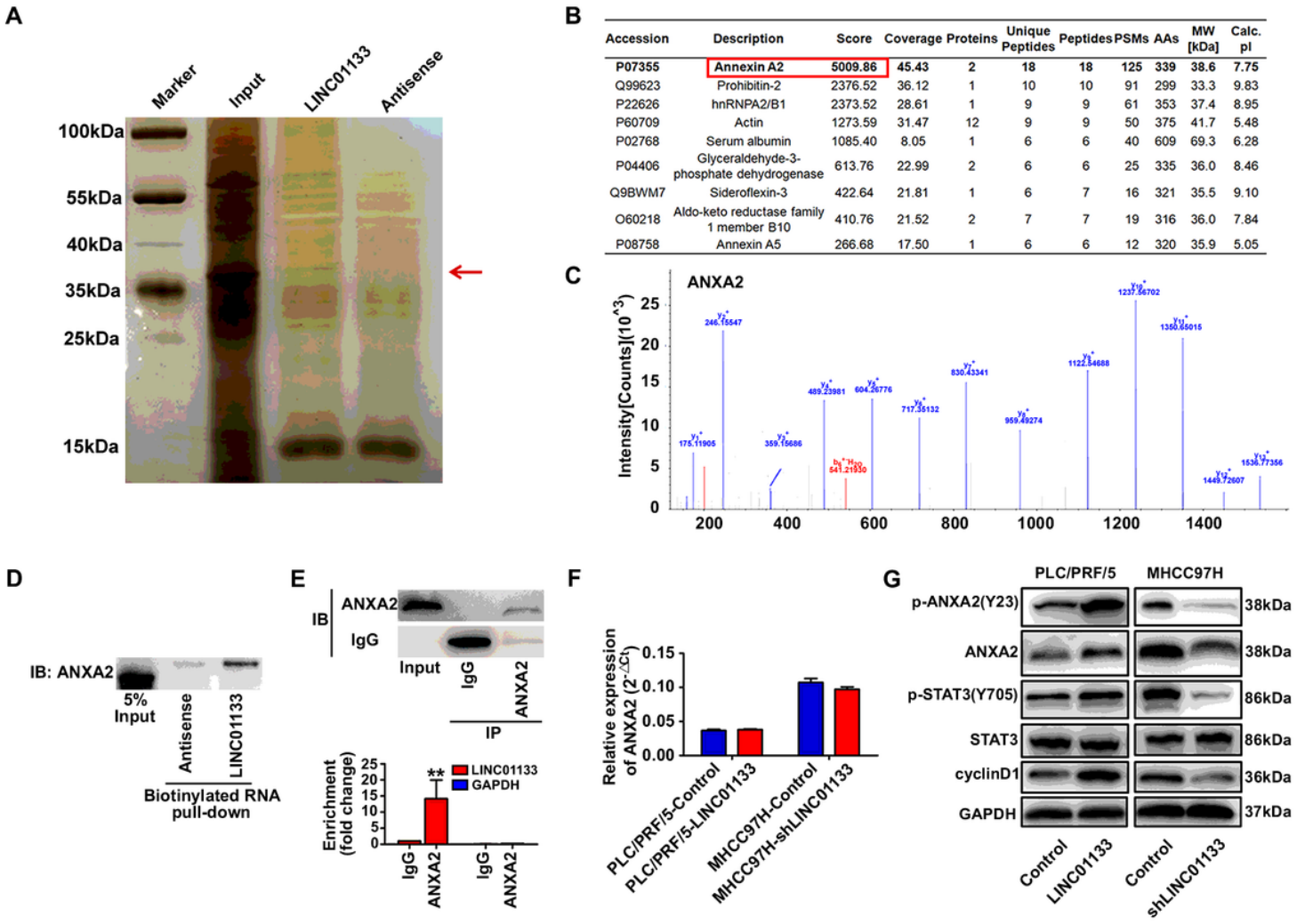

Accession	Description	Score	Coverage	Proteins	Unique Peptides	Peptides	PSMs	AAs	MW [kDa]	Calc. pI
P07355	Annexin A2	5009.86	45.43	2	18	18	125	339	38.6	7.75
Q99623	Prohibitin-2	2376.52	36.12	1	10	10	91	299	33.3	9.83
P22626	hnRNPA2/B1	2373.52	28.61	1	9	9	61	353	37.4	8.95
P60709	Actin	1273.59	31.47	12	9	9	50	375	41.7	5.48
P02768	Serum albumin	1085.40	8.05	1	6	6	40	609	69.3	6.28
P04406	Glyceraldehyde-3-phosphate dehydrogenase	613.76	22.99	2	6	6	25	335	36.0	8.46
Q9BWM7	Sideroflexin-3	422.64	21.81	1	6	7	16	321	35.5	9.10
O60218	Aldo-keto reductase family 1 member B10	410.76	21.52	2	7	7	19	316	36.0	7.84
P08758	Annexin A5	266.68	17.50	1	6	6	12	320	35.9	5.05

Figure 5

LINC01133 interacts with ANXA2 in HCC cells. (A) RNA pull-down assay was conducted to identify the proteins that physically interact with LINC01133. After silver staining, the bands around 35 kDa (red arrow) were cut and analyzed by mass spectrometry. (B) The top 9 selected proteins that potentially interact with LINC01133 are shown. (C) The secondary mass spectrum of ANXA2 identified by mass spectrometry. (D) Western blot analysis of LINC01133-bound ANXA2 from the RNA pull-down assay. (E) RNA immunoprecipitation (RIP) was performed to verify LINC01133-ANXA2 interaction. qRT-PCR was conducted to detect LINC01133 enrichment. IgG protein and GAPDH were used as negative controls for RIP and qRT-PCR, respectively. **P < 0.01. (F) qRT-PCR was conducted to measure mRNA levels of ANXA2 in LINC01133-overexpressing PLC/PRF/5 cells and LINC01133-silenced MHCC97H cells. GAPDH was used as an internal reference. (G) Western blot analysis was used to assess protein expression of ANXA2, p-ANXA2, STAT3, p-STAT3 and cyclinD1 following stable up-regulation or down-regulation of LINC01133. GAPDH was used as an internal control. Data are shown as the mean ± standard deviation and are representative of three independent experiments.

Supplementary Files

This is a list of supplementary files associated with this preprint. Click to download.

- FigureS1.tif
- FigureS2.tif
- LINC01133Supplementarytables.docx
- LINC01133SupplementaryInformation.docx
- LINC01133Supplementaryfigurelegends.docx